

doi:10.11835/j.issn.1674-4764.2018.06.007



分数导数 Kelvin 粘弹性土中管桩的扭转振动

刘林超, 闫启方, 牛洁楠

(信阳师范学院 建筑与土木工程学院, 河南 信阳 464000)

摘要:将管桩桩周土和桩芯土均看作粘弹性介质,同时运用分数导数 Kelvin 粘弹性本构模型描述桩周土和桩芯土的应力-应变关系。仅考虑桩周土和桩芯土的环向位移,通过 Fourier 变换和分离变量法求解了桩周和桩芯分数导数 Kelvin 粘弹性土的扭转振动。考虑桩周土和桩芯土对管桩的作用力,建立了分数导数 Kelvin 粘弹性土中管桩的扭转振动方程,通过求解管桩的扭转振动得到了频率域内管桩桩顶的扭转复刚度。结果表明:桩周土本构模型参数 α_1 和 T_{b1} 对管桩的扭转振动有一定的影响,而桩芯土的本构模型参数 α_2 和 T_{b2} 对管桩扭转振动的影响与频率有关;桩芯土与桩周土剪切模量比 μ 小于 1 且 μ 较大时,扭转复刚度实部和虚部随频率变化曲线波动较大,而 μ 大于 1 时其对管桩扭转振动的影响很小;管桩壁厚、长径比和管桩与土体的剪切模量比 G_p 对管桩的扭转影响较大。

关键词:粘弹性;分数导数;Fourier 变换;扭转振动;复刚度

中图分类号:TU473.16 **文献标志码:**A **文章编号:**1674-4764(2018)06-0046-07

Torsional vibration of a pipe pile in soil described by fractional derivative Kelvin viscoelastic model

Liu Linchao, Yan Qifang, Niu Jienan

(School of Architecture and Civil Engineering, Xinyang Normal University, Xinyang 464000, Henan, P. R. China)

Abstract: The soil around the pipe pile and pile core soil are regarded as viscoelastic medium, and the stress-strain relationship for them are described by fractional derivative Kelvin viscoelastic constitutive model. The torsional vibrations are solved by Fourier transformation and separation variable method by considering the circumferential displacement of the soil only. Considering the forces acting on the pipe piles, the torsional vibration in the fractional derivative Kelvin viscoelastic soil is established. The torsional complex stiffness at pipe pile head is obtained by solving the torsional vibration of the pipe pile. The results show that the model soil parameters α_1 and T_{b1} have certain influence on the torsional vibration while the influence of the pile core soil model parameters α_2 and T_{b2} is related to frequency. The curves of real and imaginary parts of torsional complex stiffness with frequency fluctuate more greatly when the shear

收稿日期:2017-10-10

基金项目:国家自然科学基金(U1504505);河南省科技发展计划(142102210063);河南省高等学校重点科研项目(19B560008);信阳师范学院南湖学者奖励计划青年项目(201506)

作者简介:刘林超(1979-),男,博士,副教授,主要从事多孔介质理论、粘弹性理论、桩基动力学研究,E-mail:llc109@126.com。

Received:2017-10-10

Foundation item: National Natural Science Foundation of China (No. U1504505); Development of Science and Technology Plan Project of Henan Province (No. 142102210063); Key Scientific Research Project of Henan Province (No. 19B560008); Nanhu Scholars Program for Young Scholars of XYNU (No. 201506)

Author brief: Liu Linchao (1979-), PhD, associate professor, main research interests: theory of porous medium, viscoelastic theory and pile dynamics, E-mail: llc109@126.com.

modulus ratio μ is larger and $\mu < 1$, and the influence of shear modulus ratio μ on the torsional vibration of pipe pile is very small when $\mu > 1$. Wall thickness, length diameter ratio of pipe pile, as well as the shear modulus of pipe pile and soil have great influence on the torsional vibration of pipe pile.

Keywords: viscoelastic; fractional derivative; Fourier transform; torsional vibration; complex stiffness

桩土动力相互作用问题作为一个研究热点得到了众多学者的关注和重视,但无论是研究实芯桩还是管桩的振动特性,对土体本构模型的选取十分关键,这关系到土体力学行为的描述与实际工况的符合程度,通常情况是将土体视为弹性或粘弹性介质,将土体视为弹性介质,Novak 等^[1]和 Nogami 等^[2]较早地对实芯桩的振动进行了研究,王国才等^[3]借助于积分方程研究了均质弹性地基中单桩的扭转振动问题,Lü 等^[4]利用 Rayleigh-Love 杆理论和桩土摩擦模型对层状土中桩的纵向振动进行了研究,刘林超等^[5]将桩周土、桩芯土和管桩视为轴对称模型研究了弹性土中管桩的纵向振动,栾鲁宝等^[6]在考虑桩体剪切变形的情况下得到了 PCC 桩水平振动的解析解,吴文兵等^[7]采用 Rayleigh-Love 动力杆件模型和附加质量模型建立了桩侧土-管桩-土塞系统的纵向振动控制方程,同时,运用积分变换和阻抗函数传递技术给出了频域内任意荷载形式下管桩桩顶速度响应的解析解;将土体视为粘弹性介质,Novak^[8]给出了桩基的动力刚度和阻尼,Yao 等^[9]研究了粘弹性 Winkler 地基中单桩在水平循环荷载作用下的振动问题,周绪红等^[10]在考虑轴力作用的情况下研究了粘弹性介质中桩基的动力问题,杨骁等^[11]采用三维轴对称模型得到了粘弹性端承桩的轴对称解析解,郑长杰等^[12-13]对单相和饱和粘弹性土中大直径管桩的水平振动进行了研究,吴文斌等^[14]利用虚土桩模型研究了均质粘弹性地基中桩土纵向耦合振动问题。需要指出,将桩周土或桩芯土视为弹性介质则不能考虑土体的粘性性质,将土视为粘弹性介质较为符合工程实际,但需选择合理的土体粘弹性本构模型。

当将桩周土或桩芯土视为粘弹性介质时,合理的本构关系对于土体力学行为的准确描述至关重要。目前,对于粘弹性材料应力-应变关系的刻画主要是采用经典的粘弹性模型。然而,对于经典的粘弹性本构模型,整数阶微分算子的性质决定其蠕变柔量和松弛模量一般只能通过指数函数的组合得到,且通过取消高阶的微分项或者降低本构模型的应用范围来精确拟合实验数据^[15]。随着分数阶微分和分数阶积分的发展,借助于分数导数理论建立起来的分数导数粘弹性本构模型由于具有确定模型需要较少的实验参数和能在较宽的频率范围内拟合

材料的力学行为而得到了广泛的应用。将桩周土视为粘弹性介质并采用分数导数粘弹性模型来描述其应力-应变关系,刘林超等^[16-17]、闻敏杰等^[18]研究了实芯桩的水平、竖向和扭转振动问题。本文将桩周土和桩芯土都利用分数导数 Kelvin 粘弹性本构模型来描述,研究分数导数 Kelvin 粘弹性土中管桩的扭转振动特性。

1 数学模型与土体运动方程

图 1 为粘弹性土与端承管桩的动力相互作用模型,管桩桩顶作用一集中扭转荷载 $T(t)$,粘弹性土层厚度和管桩长度均为 H ,管桩外半径和内半径分别为 r_1 和 r_2 。为了建立管桩与粘弹性土体的动力相互作用模型,假设管桩桩芯土体和桩周土体均为粘弹性土体,且桩芯土和桩周土均与管桩完全接触;管桩底部为基岩,管桩底端为固定端;管桩、桩周土和桩芯土均为小变形。

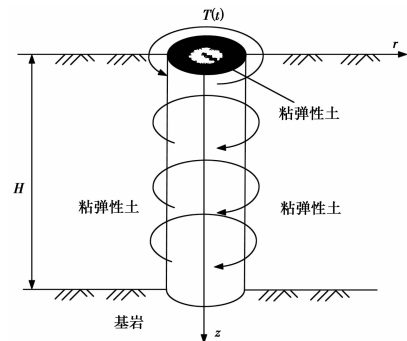


图 1 粘弹性土-管桩扭转相互作用模型

Fig. 1 Torsional interaction model of viscoelastic soil-pipe pile

这里以 $\beta=1$ 代表桩周粘弹性土体, $\beta=2$ 代表桩芯粘弹性土体,可以建立轴对称坐标下桩周粘弹性土和桩芯粘弹性土的运动方程和几何方程分别为^[19]

$$\begin{cases} \frac{\partial \sigma_{r\beta}}{\partial r} + \frac{1}{r} \frac{\partial \sigma_{r\theta\beta}}{\partial \theta} + \frac{\partial \sigma_{rz\beta}}{\partial z} + \frac{\sigma_{r\beta} - \sigma_{\theta\beta}}{r} = \rho_{\beta} \frac{\partial^2 u_{r\beta}}{\partial t^2} \\ \frac{\partial \sigma_{\theta\beta}}{\partial r} + \frac{1}{r} \frac{\partial \sigma_{\theta\theta\beta}}{\partial \theta} + \frac{\partial \sigma_{\theta z\beta}}{\partial z} + 2 \frac{\sigma_{\theta\beta}}{r} = \rho_{\beta} \frac{\partial^2 u_{\theta\beta}}{\partial t^2} \\ \frac{\partial \sigma_{rz\beta}}{\partial r} + \frac{1}{r} \frac{\partial \sigma_{z\theta\beta}}{\partial \theta} + \frac{\partial \sigma_{zz\beta}}{\partial z} + \frac{\sigma_{rz\beta}}{r} = \rho_{\beta} \frac{\partial^2 u_{z\beta}}{\partial t^2} \end{cases} \quad (1)$$

$$\epsilon_{\beta} = \frac{1}{2} (\text{grad} u_{\beta} + \text{grad}^T u_{\beta}) \quad (2)$$

式中: $\sigma_{rr}, \sigma_{\theta\theta}, \sigma_{zz}$ 分别为粘弹性土体径向应力、环向应力和剪切应力, $u_{rr}, u_{\theta\theta}, u_{zz}$ 分别为粘弹性土体的径向位移、环向位移和竖向位移, ρ_β 为粘弹性土体的密度, \mathbf{u}_β 为粘弹性土体的位移张量。

为了更合理地考虑桩周土和桩芯土的粘弹性性质, 采用分数导数 Kelvin 粘弹性模型构建桩周土和桩芯土的三维本构关系, 即^[20]

$$[1 + a_{\beta\beta} \frac{d^{\alpha_\beta}}{dt^{\alpha_\beta}}] \boldsymbol{\sigma}_\beta = [1 + b_{\beta\beta} \frac{d^{\alpha_\beta}}{dt^{\alpha_\beta}}] [\lambda(\boldsymbol{\varepsilon}_\beta \cdot \mathbf{I})\mathbf{I} + 2\mu_\beta \boldsymbol{\varepsilon}_\beta] \quad (3)$$

式中: $\boldsymbol{\sigma}_\beta, \boldsymbol{\varepsilon}_\beta$ 分别为粘弹性土体的应力与应变张量, \mathbf{I} 为单位矩阵, $a_{\beta\beta}, b_{\beta\beta}, \alpha_\beta$ 代表粘弹性土体的本构模型参量, 模型参量可以借助于土体蠕变试验数据拟合得到, λ_β, μ_β 代表粘弹性土体的拉梅常数, $D^{\alpha_\beta} = \frac{d^{\alpha_\beta}}{dt^{\alpha_\beta}} = \frac{1}{\Gamma(1-\alpha)} \frac{d}{dt} \int_0^t \frac{x(\tau)}{(t-\tau)^{\alpha}} d\tau$ 为 $\alpha_\beta (0 < \alpha_\beta < 1)$ 阶 Riemann-Liouville 分数阶导数^[21], 其中 $\Gamma(u)$ 代表 Gamma 函数。

对于粘弹性土体中管桩的扭转简谐振动问题, 为了简化计算, 这里只考虑桩周土和桩芯土的环向位移 $u_{\theta\theta}$, 其他位移忽略不计, 在此情况下由式(1)~式(3)可以建立分数导数粘弹性土体以环向位移表示的桩周土和桩芯土的扭转振动控制方程为

$$\begin{aligned} \mu_\beta (1 + b_{\beta\beta} \frac{d^{\alpha_\beta}}{dt^{\alpha_\beta}}) (\frac{\partial^2 \mathbf{u}_{\theta\theta}}{\partial r^2} + \frac{1}{r} \frac{\partial \mathbf{u}_{\theta\theta}}{\partial r} - \frac{\mathbf{u}_{\theta\theta}}{r^2} + \frac{\partial^2 \mathbf{u}_{\theta\theta}}{\partial z^2}) \\ = \rho_\beta (1 + a_{\beta\beta} \frac{d^{\alpha_\beta}}{dt^{\alpha_\beta}}) \frac{\partial^2 \mathbf{u}_{\theta\theta}}{\partial t^2} \end{aligned} \quad (4)$$

很明显, 式(4)即适用于分数导数 Kelvin 粘弹性土体的扭转振动, 也适用于经典 Kelvin ($\alpha_\beta = 1$) 粘弹性土体以及弹性土体 ($a_{\beta\beta} = b_{\beta\beta} = 0$) 的情形。

2 分数导数 Kelvin 粘弹性土层的扭转振动求解

令式(4)中 $\beta=1$ 和 $\beta=2$ 可得分数导数 Kelvin 粘弹性桩周土和桩芯土的扭转振动方程分别为

$$\begin{aligned} \mu_1 (1 + b_{11} \frac{d^{\alpha_1}}{dt^{\alpha_1}}) (\frac{\partial^2 u_{\theta 1}}{\partial r^2} + \frac{1}{r} \frac{\partial u_{\theta 1}}{\partial r} - \frac{u_{\theta 1}}{r^2} + \frac{\partial^2 u_{\theta 1}}{\partial z^2}) \\ = \rho_1 (1 + a_{11} \frac{d^{\alpha_1}}{dt^{\alpha_1}}) \frac{\partial^2 u_{\theta 1}}{\partial t^2} \end{aligned} \quad (5)$$

$$\begin{aligned} \mu_2 (1 + b_{22} \frac{d^{\alpha_2}}{dt^{\alpha_2}}) (\frac{\partial^2 u_{\theta 2}}{\partial r^2} + \frac{1}{r} \frac{\partial u_{\theta 2}}{\partial r} - \frac{u_{\theta 2}}{r^2} + \frac{\partial^2 u_{\theta 2}}{\partial z^2}) \\ = \rho_2 (1 + a_{22} \frac{d^{\alpha_2}}{dt^{\alpha_2}}) \frac{\partial^2 u_{\theta 2}}{\partial t^2} \end{aligned} \quad (6)$$

对方程(5)和式(6)两端分别进行 Fourier 变换可得

$$\begin{aligned} \mu_1 [1 + (i\omega b_1)^{\alpha_1}] (\frac{\partial^2 \bar{u}_{\theta 1}}{\partial r^2} + \frac{1}{r} \frac{\partial \bar{u}_{\theta 1}}{\partial r} - \frac{\bar{u}_{\theta 1}}{r^2} + \frac{\partial^2 \bar{u}_{\theta 1}}{\partial z^2}) \\ = -\rho_1 \omega^2 [1 + (i\omega a_1)^{\alpha_1}] \bar{u}_{\theta 1} \end{aligned} \quad (7)$$

$$\begin{aligned} \mu_2 [1 + (i\omega b_2)^{\alpha_2}] (\frac{\partial^2 \bar{u}_{\theta 2}}{\partial r^2} + \frac{1}{r} \frac{\partial \bar{u}_{\theta 2}}{\partial r} - \frac{\bar{u}_{\theta 2}}{r^2} + \frac{\partial^2 \bar{u}_{\theta 2}}{\partial z^2}) \\ = -\rho_2 \omega^2 [1 + (i\omega a_2)^{\alpha_2}] \bar{u}_{\theta 2} \end{aligned} \quad (8)$$

式中: $\bar{u}_{\theta 1}$ 和 $\bar{u}_{\theta 2}$ 分别为 $u_{\theta 1}, u_{\theta 2}$ 的 Fourier 变换。令 $\bar{r} = \frac{r}{r_1}, \bar{z} = \frac{z}{r_1}, \bar{\omega} = \frac{r_1 \omega}{v_{s1}}, v_{s1} = \sqrt{\mu_1 / \rho_1}, \bar{u}_{\theta 1} = \frac{\bar{u}_{\theta 1}}{r_1}, \bar{u}_{\theta 2} = \frac{\bar{u}_{\theta 2}}{r_1}, T_{a1} = a_1 v_{s1} / r_1, T_{b1} = b_1 v_{s1} / r_1, \mu = \frac{\mu_2}{\mu_1}, \rho = \frac{\rho_2}{\rho_1}, T_{a2} = a_2 v_{s1} / r_1, T_{b2} = b_2 v_{s1} / r_1$, 则式(7)和式(8)

整理为

$$\frac{\partial^2 \bar{u}_{\theta 1}}{\partial \bar{r}^2} + \frac{1}{\bar{r}} \frac{\partial \bar{u}_{\theta 1}}{\partial \bar{r}} - \frac{\bar{u}_{\theta 1}}{\bar{r}^2} + \frac{\partial^2 \bar{u}_{\theta 1}}{\partial \bar{z}^2} + q_1 \bar{u}_{\theta 1} = 0 \quad (9)$$

$$\frac{\partial^2 \bar{u}_{\theta 2}}{\partial \bar{r}^2} + \frac{1}{\bar{r}} \frac{\partial \bar{u}_{\theta 2}}{\partial \bar{r}} - \frac{\bar{u}_{\theta 2}}{\bar{r}^2} + \frac{\partial^2 \bar{u}_{\theta 2}}{\partial \bar{z}^2} + q_2 \bar{u}_{\theta 2} = 0 \quad (10)$$

式中: $q_1 = \frac{\bar{\omega}^2 [1 + (i\bar{\omega} T_{a1})^{\alpha_1}]}{1 + (i\bar{\omega} T_{b1})^{\alpha_1}}, q_2 = \frac{\bar{\omega}^2 [1 + (i\bar{\omega} T_{a2})^{\alpha_2}]}{\mu [1 + (i\bar{\omega} T_{b2})^{\alpha_2}]}$ 。

为了求解式(9)和式(10), 令 $\bar{u}_{\theta 1} = R_1(\bar{r})Z_1(\bar{z}), \bar{u}_{\theta 2} = R_2(\bar{r})Z_2(\bar{z})$, 对式(9)和式(10)分离变量可得

$$\frac{\partial^2 R_1}{\partial \bar{r}^2} + \frac{1}{\bar{r}} \frac{\partial R_1}{\partial \bar{r}} - (\frac{1}{\bar{r}^2} + \beta_1^2) R_1 = 0 \quad (11)$$

$$\frac{\partial^2 Z_1}{\partial \bar{z}^2} + m_1^2 Z_1 = 0 \quad (12)$$

$$\frac{\partial^2 R_2}{\partial \bar{r}^2} + \frac{1}{\bar{r}} \frac{\partial R_2}{\partial \bar{r}} - (\frac{1}{\bar{r}^2} + \beta_2^2) R_2 = 0 \quad (13)$$

$$\frac{\partial^2 Z_2}{\partial \bar{z}^2} + m_2^2 Z_2 = 0 \quad (14)$$

式中: $\beta_1^2 = m_1^2 - q_1, \beta_2^2 = m_2^2 - q_2$ 。由式(11)~式(14)可将桩周和桩芯粘弹性土的环向位移分别表示为

$$\begin{aligned} \bar{u}_{\theta 1} = [A_1 K_1(\beta_1 \bar{r}) + B_1 I_1(\beta_1 \bar{r})] \cdot \\ [C_1 \sin(m_1 \bar{z}) + D_1 \cos(m_1 \bar{z})] \end{aligned} \quad (15)$$

$$\begin{aligned} \bar{u}_{\theta 2} = [A_2 K_1(\beta_2 \bar{r}) + B_2 I_1(\beta_2 \bar{r})] \cdot \\ [C_2 \sin(m_2 \bar{z}) + D_2 \cos(m_2 \bar{z})] \end{aligned} \quad (16)$$

式(11)和式(14)中, $I_1(\cdot), K_1(\cdot)$ 分别为 1 阶第 1 和第 2 类虚宗量贝塞尔函数, $A_1, B_1, C_1, D_1, A_2, B_2, C_2, D_2$ 为待定系数。

考虑问题的边界条件, 由 $\bar{u}_{\theta 1} |_{\bar{r} \rightarrow \infty} = 0$, 可得 $B_1 = 0$; 当 $\bar{r} \rightarrow 0$ 时, $\bar{u}_{\theta 2}$ 为有限值, 所以 $A_2 = 0$; 由于桩周土和桩芯土体上表面自由, 则 $\sigma_{z\theta} |_{z=0} = 0, \sigma_{\theta z} |_{z=0} = 0$, 由此可得 $C_1 = 0, C_2 = 0$; 当假设管桩桩底端为基岩时, 则有 $\bar{u}_{\theta 1}(\delta) = 0, \bar{u}_{\theta 2}(\delta) = 0$, 这里 $\delta = H/r_1$, 由此可得

$$\cos(m_1\delta) = 0, \cos(m_2\delta) = 0 \quad (17)$$

由式(17)可得到

$$m_{1n} = m_{2n} = \gamma_n = \frac{(2n-1)\pi}{2\delta}, n = 1, 2, \dots, \infty \quad (18)$$

则分数阶 Kelvin 粘弹性桩周土和桩芯土的回向位移可以分别用级数表示为

$$\bar{u}_{1\theta} = \sum_{n=1}^{\infty} A_{1n} K_1(\beta_{1n} \bar{r}) \cos(\gamma_n \bar{z}) \quad (19)$$

$$\bar{u}_{2\theta} = \sum_{n=1}^{\infty} B_{2n} I_1(\beta_{2n} \bar{r}_2) \cos(\gamma_n \bar{z}) \quad (20)$$

式中: A_{2n} 、 B_{2n} 为待定系数。考虑分数阶 Kelvin 粘弹性体本构关系式(3), 并对其进行 Fourier 变换, 则有

$$\bar{\sigma}_{r\theta 1} = \zeta_1 \left(\frac{\partial \bar{u}_{\theta 1}}{\partial r} - \frac{\bar{u}_{\theta 1}}{r} \right) = \zeta_1 \sum_{n=1}^{\infty} A_{1n} [-\beta_{1n} K_0(\beta_{1n} \bar{r}) - \frac{2}{r} K_1(\beta_{1n} \bar{r})] \cos(\gamma_n \bar{z}) \quad (21)$$

$$\bar{\sigma}_{r\theta 2} = \mu \zeta_2 \left(\frac{\partial \bar{u}_{\theta 2}}{\partial r} - \frac{\bar{u}_{\theta 2}}{r} \right) = \mu \zeta_2 \sum_{n=1}^{\infty} B_{2n} [\beta_{2n} I_0(\beta_{2n} \bar{r}_2) - \frac{2}{r} I_1(\beta_{2n} \bar{r}_2)] \cos(\gamma_n \bar{z}) \quad (22)$$

$$\text{式中: } \zeta_1 = \frac{1 + (i\omega T_{b1})^{a_1}}{1 + (i\omega T_{a1})^{a_1}}, \zeta_2 = \frac{1 + (i\omega T_{b2})^{a_2}}{1 + (i\omega T_{a2})^{a_2}}, \bar{\sigma}_{r\theta 1} =$$

$\bar{\sigma}_{r\theta 1}$, $\bar{\sigma}_{r\theta 2} = \frac{\bar{\sigma}_{r\theta 2}}{\mu}$, $\bar{\sigma}_{r\theta 1}$ 、 $\bar{\sigma}_{r\theta 2}$ 分别为应力 $\sigma_{r\theta 1}$ 、 $\sigma_{r\theta 2}$ 的 Fourier 变换。由式(21)和式(22)可知, 在管桩-土接触面处桩周土和桩芯土对管桩的切向作用力分别为

$$P_1 = -\bar{\sigma}_{r\theta 1} |_{r=1} =$$

$$\zeta_1 \sum_{n=1}^{\infty} A_{1n} [\beta_{1n} K_0(\beta_{1n}) + 2K_1(\beta_{1n})] \cos(\gamma_n \bar{z}) \quad (23)$$

$$P_2 = \bar{\sigma}_{r\theta 2} |_{r=r_2} =$$

$$\mu \zeta_2 \sum_{n=1}^{\infty} B_{2n} [\beta_{2n} I_0(\beta_{2n} \bar{r}_2) - \frac{2}{r_2} I_1(\beta_{2n} \bar{r}_2)] \cos(\gamma_n \bar{z}) \quad (24)$$

式中: $P_1 = \frac{\bar{P}_1}{\mu_1}$, $P_2 = \frac{\bar{P}_2}{\mu_1}$, \bar{P}_1 和 \bar{P}_2 分别为 \tilde{P}_1 和 \tilde{P}_2 的 Fourier 变换, \tilde{P}_1 和 \tilde{P}_2 分别为管桩-土接触面处桩周土和桩芯土对管桩的切向作用力。

3 分数阶 Kelvin 粘弹性土端承管桩的扭转振动求解

以管桩桩身微元作为研究对象可以建立分数阶 Kelvin 粘弹性土中管桩的扭转振动控制方程为

$$\tilde{G}_p J_p \frac{\partial^2 \bar{\theta}}{\partial z^2} - 2\pi r_1^2 \tilde{P}_1 - 2\pi r_2^2 \tilde{P}_2 = \rho_p J_p \frac{\partial^2 \bar{\theta}}{\partial t^2} \quad (25)$$

式中: \tilde{G}_p 为管桩桩身的剪切模量, ρ_p 为管桩桩身的

密度, $\bar{\theta}$ 为管桩的扭转角, J_p 为管桩桩身截面的极惯性矩, 且 $J_p = \pi(r_1^4 - r_2^4)/2$, \tilde{P}_1 、 \tilde{P}_2 为桩周土和桩芯土对管桩桩身的剪切作用力。对式(25)两端进行 Fourier 变换, 两端同除以 μ_1 , 同时考虑桩周土和桩芯土对管桩的剪切作用力式(23)和式(24), 得

$$\frac{\partial^2 \bar{\theta}}{\partial z^2} - \lambda^2 \bar{\theta} = \frac{4\zeta_1}{G_p(1-r_2^4)} \sum_{n=1}^{\infty} A_{1n} [\beta_{1n} K_0(\beta_{1n}) + 2K_1(\beta_{1n})] \cos(\gamma_n \bar{z}) + \frac{4r_2^2 \mu \zeta_2}{G_p(1-r_2^4)} \sum_{n=1}^{\infty} B_{2n} [\beta_{2n} I_0(\beta_{2n} \bar{r}_2) - \frac{2}{r_2} I_1(\beta_{2n} \bar{r}_2)] \cos(\gamma_n \bar{z}) \quad (26)$$

式(19)中, $G_p = \frac{\tilde{G}_p}{\mu_1}$, $\rho_p = \frac{\rho_p}{\rho_1}$, $\lambda^2 = -\frac{\rho_p \omega^2}{G_p}$, $\bar{\theta}$ 为 $\bar{\theta}$ 的 Fourier 变换。端承管桩桩底和桩顶以及管桩与桩芯土和桩周土接触面处的边界条件为

$$\bar{\theta}(\bar{z}) |_{\bar{z}=\delta} = 0, \frac{\partial \bar{\theta}(\bar{z})}{\partial \bar{z}} \Big|_{\bar{z}=0} = -\frac{\bar{T}}{G_p(1-r_2^4)} \quad (27)$$

$$\bar{u}_{1\theta} = \bar{\theta}, \bar{u}_{2\theta} = \bar{r}_2 \bar{\theta} \quad (28)$$

式中: $\bar{T} = 2\tilde{T}/\mu_1 \pi r_1^3$, \tilde{T} 为 $T(t)$ 的 Fourier 变换。由边界条件式(27)可求得

$$\bar{\theta} = -\frac{\bar{T}_0 e^{\bar{z}}}{\lambda G_p(1-r_2^4)(1+e^{2\delta})} + \frac{e^{2\delta} \bar{T}_0 e^{-\lambda \bar{z}}}{\lambda G_p(1-r_2^4)(1+e^{2\delta})} - \frac{4\zeta_1}{G_p(1-r_2^4)} \sum_{n=1}^{\infty} A_{1n} [\beta_{1n} K_0(\beta_{1n}) + 2K_1(\beta_{1n})] \cdot \frac{\cos(\gamma_n \bar{z})}{\gamma_n^2 + \lambda^2} - \frac{4r_2^2 \mu \zeta_2}{G_p(1-r_2^4)} \sum_{n=1}^{\infty} B_{2n} [\beta_{2n} I_0(\beta_{2n} \bar{r}_2) - \frac{2}{r_2} I_1(\beta_{2n} \bar{r}_2)] \frac{\cos(\alpha_n \bar{z})}{\gamma_n^2 + \lambda^2} \quad (29)$$

考虑管桩与桩周土和桩芯土接触面边界条件式(28), 由式(19)、式(20)可得

$$\sum_{n=1}^{\infty} B_{2n} I_1(\beta_{2n} \bar{r}_2) \cos(\gamma_n \bar{z}) = \bar{r}_2 \sum_{n=1}^{\infty} A_{1n} K_1(\beta_{1n}) \cos(\gamma_n \bar{z}) \quad (30)$$

$$\sum_{n=1}^{\infty} A_{1n} K_1(\beta_{1n}) \cos(\alpha_n \bar{z}) = -\frac{\bar{T}_0 e^{\bar{z}}}{\lambda G_p(1-r_2^4)(1+e^{2\delta})} + \frac{e^{2\delta} \bar{T}_0 e^{-\lambda \bar{z}}}{\lambda G_p(1-r_2^4)(1+e^{2\delta})} - \frac{4\zeta_1}{G_p(1-r_2^4)} \sum_{n=1}^{\infty} A_{1n} [\beta_{1n} K_0(\beta_{1n}) + 2K_1(\beta_{1n})] \frac{\cos(\gamma_n \bar{z})}{\gamma_n^2 + \lambda^2} - \frac{4r_2^2 \mu \zeta_2}{G_p(1-r_2^4)} \sum_{n=1}^{\infty} B_{2n} [\beta_{2n} I_0(\beta_{2n} \bar{r}_2) - \frac{2}{r_2} I_1(\beta_{2n} \bar{r}_2)] \frac{\cos(\gamma_n \bar{z})}{\gamma_n^2 + \lambda^2} \quad (31)$$

式(30)和式(31)两端分别同乘以 $\cos(\alpha_n \bar{z})$, 进行三角函数正交性运算, 然后求解方程组有

$$B_{2n} = \frac{\bar{r}_2 K_1(\beta_{1n})}{I_1(\beta_{2n} \bar{r}_2)} A_{1n} \quad (32)$$

$$A_{1n} = \frac{2I_1(\beta_{2n}\bar{r}_2)T_0}{\psi_n} \quad (33)$$

式中: $\psi_n = \delta\bar{G}_p(1-\bar{r}_2^4)(\lambda^2 + \alpha_n^2)K_1(\beta_{1n})I_1(\beta_{2n}\bar{r}_2) + 4\zeta_1\delta I_1(\beta_{2n}\bar{r}_2)[\beta_{1n}K_0(\beta_{1n}) + 2K_1(\beta_{1n})] + 4\bar{r}_2\mu\zeta_2\delta K_1(\beta_{1n})[\beta_{2n}\bar{r}_2 I_0(\beta_{2n}\bar{r}_2) - 2I_1(\beta_{2n}\bar{r}_2)]$ 。

由此可得分数导数 Kelvin 粘弹性土中管桩扭转振动的扭转角为

$$\bar{\theta}(0) = \bar{u}_{1\theta}|_{\bar{r}=1} = \sum_{n=1}^{\infty} \frac{2I_1(\beta_{2n}\bar{r}_2)K_1(\beta_{1n})T_0}{\psi_n} \quad (34)$$

进而可以得到频率域内分数导数 Kelvin 粘弹性土管桩桩顶的扭转复刚度

$$K = \frac{\bar{T}(0)}{\bar{\theta}(0)} = \frac{1}{-\sum_{n=1}^{\infty} \frac{2I_1(\beta_{2n}\bar{r}_2)K_1(\beta_{1n})}{\psi_n}} \quad (35)$$

4 数值算例分析与讨论

为了研究分数导数 Kelvin 粘弹性土中管桩的扭转振动响应特性,根据式(35)得到的管桩桩顶扭转复刚度编写计算程序并进行数值分析,图 2—图 11 为:管桩与桩周土剪切模量比 $G_p=2000$,分数导数阶数 $\alpha_1=\alpha_2=0.5$,管桩长径比 $\delta=20$,管桩与桩周土密度比 $\rho_p/\rho_1=2.0$,土体分数导数本构模型参数 $T_{a1}=T_{a2}=2.0$, $T_{b1}=T_{b2}=4.0$,桩芯土与桩周土剪切模量比 $\mu=1.0$,以上参量的取值是在桩身混凝土和土体实际常用参量值的基础上确定的,土体分数导数模型参数可以通过实验数据拟合的方法得到^[22]。图 2 给出了管桩扭转振动的分数导数粘弹性解、经典粘弹性解和弹性解的对比,可以看出,分数导数粘弹性解可退化到经典粘弹性和弹性解的情况,间接说明采用分数导数粘弹性模型分析管桩扭转振动的可行性和正确性,且弹性解的扭转复刚度要较粘弹性解大。图 3 和图 4 分别给出了桩周土和桩芯土本构关系中分数导数的阶数 α_1 、 α_2 不同时对管桩扭转复刚度的影响,可以看出,桩周土分数导数的阶数 α_1 对扭转复刚度的实部和虚部的影响相对较大,且分数导数的阶数越大,扭转复刚度实部和虚部随频率变化曲线的峰值越小;而桩芯土分数导数的阶数 α_2 对扭转复刚度的影响与频率有关,频率较低时 α_2 几乎没有影响,而高频时有一定的影响。图 5 和图 6 给出了参数 T_{b1} 和 T_{b2} 不同时复刚度随频率的变化曲线, T_{b1} 和 T_{b2} 对扭转复刚度的影响与分数导数的阶数 α_1 和 α_2 的影响规律类似,即 T_{b1} 的影响较大且 T_{b1} 越大扭转复刚度的实部和虚部随频率变化曲线的峰值越小,而 T_{b2} 的影

响与频率有关。由图 7 和图 8 可知,当桩芯土与桩周土剪切模量比 μ 大于 1 时,其对管桩桩顶扭转复刚度几乎没有影响,这可能是因为桩芯土与管桩接触面相对较小,导致增大桩芯土剪切模量时其对管桩的剪切作用力增大不明显;当 μ 小于 1 且较小时剪切模量比对管桩复刚度有一定的影响但不是太大,但当 μ 较大时扭转复刚度实部和虚部随频率变化曲线波动则较大。管桩壁厚对扭转复刚度的影响较大(如图 9),随着桩周内半径的增大,即管桩壁厚的减小,扭转复刚度实部和虚部随频率变化曲线峰值对应的频率越小,曲线波动越大。与实芯桩一样,管桩长径比(图 10)和管桩与土体的剪切模量比(图 11)对管桩的影响也较大,管桩长径比越大复刚度的实部和虚部越小,桩长较长时长径比的影响程度将减小;随着管桩与土体剪切模量比的增大,管桩桩顶复刚度实部和虚部越大,这可能是因为管桩模量较大时管桩抗扭刚度大,管桩扭转角小而导致复刚度增大。

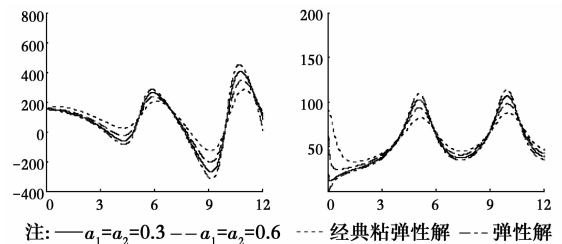


图 2 α_1, α_2 3 种模型对比分析

Fig. 2 Contrastive analysis of three models

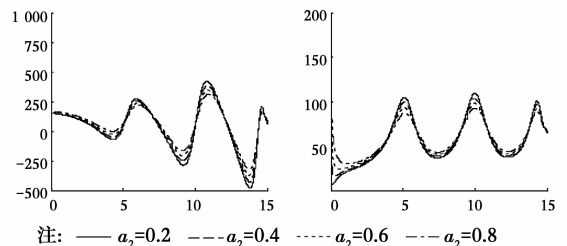


图 3 α_1 不同时桩顶扭转复刚度随频率变化曲线

Fig. 3 Curves of the torsional complex stiffness varying with frequency for different α_1

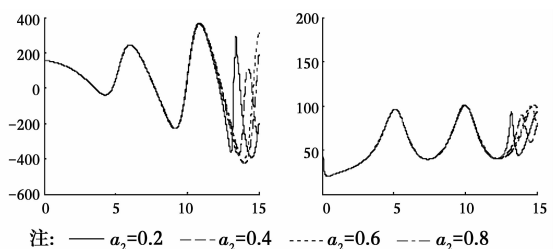
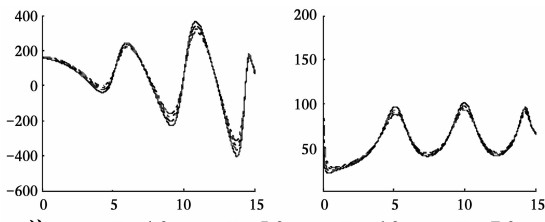


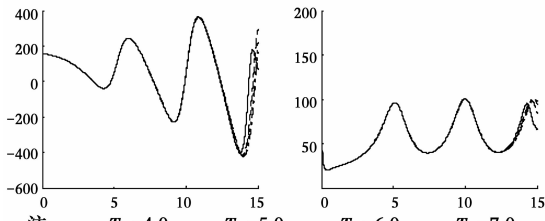
图 4 α_2 不同时桩顶扭转复刚度随频率变化曲线

Fig. 4 Curves of the torsional complex stiffness varying with frequency for different α_2



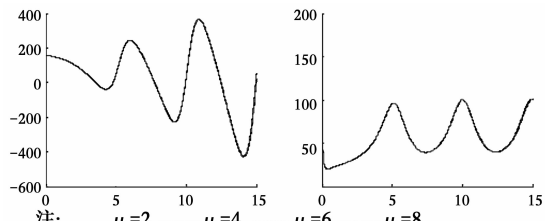
注: — $T_{b1}=4.0$ --- $T_{b1}=5.0$ $T_{b1}=6.0$ ---- $T_{b1}=7.0$

图 5 T_{b1} 不同时桩顶扭转复刚度随频率变化曲线
Fig. 5 Curves of the torsional complex stiffness varying with frequency for different T_{b1}



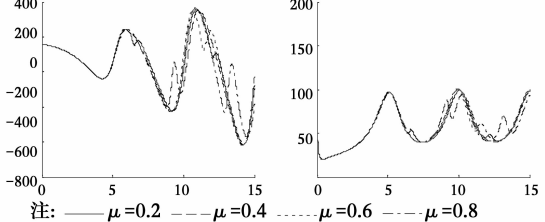
注: — $T_{b2}=4.0$ --- $T_{b2}=5.0$ $T_{b2}=6.0$ ---- $T_{b2}=7.0$

图 6 T_{b2} 不同时桩顶扭转复刚度随频率变化曲线
Fig. 6 Curves of the torsional complex stiffness varying with frequency for different T_{b2}



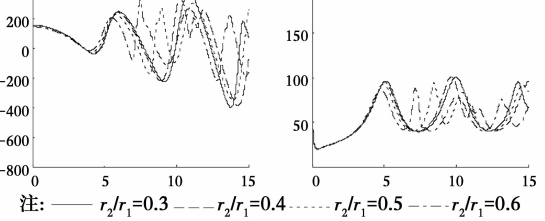
注: — $\mu=2$ --- $\mu=4$ $\mu=6$ ---- $\mu=8$

图 7 μ 不同时桩顶扭转复刚度随频率变化曲线
Fig. 7 Curves of the torsional complex stiffness varying with frequency for different μ



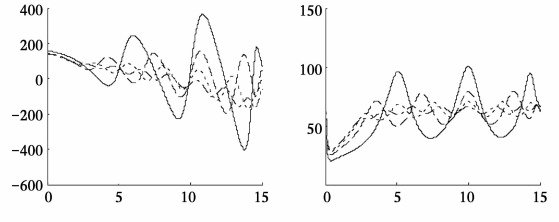
注: — $\mu=0.2$ --- $\mu=0.4$ $\mu=0.6$ ---- $\mu=0.8$

图 8 μ 不同时桩顶扭转复刚度随频率变化曲线
Fig. 8 Curves of the torsional complex stiffness varying with frequency for different μ



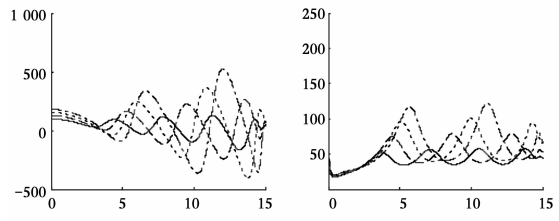
注: — $r_2/r_1=0.3$ --- $r_2/r_1=0.4$ $r_2/r_1=0.5$ ---- $r_2/r_1=0.6$

图 9 r_2/r_1 不同时桩顶扭转复刚度随频率变化曲线
Fig. 9 Curves of the torsional complex stiffness varying with frequency for different r_2/r_1



注: — $\delta=20$ --- $\delta=30$ $\delta=40$ ---- $\delta=50$

图 10 δ 不同时桩顶扭转复刚度随频率变化曲线
Fig. 10 Curves of the torsional complex stiffness varying with frequency for different δ



注: — $G_p=1\ 000$ --- $G_p=1\ 500$ $G_p=2\ 000$ ---- $G_p=2\ 500$

图 11 G_p 不同时桩顶扭转复刚度随频率变化曲线
Fig. 11 Curves of the torsional complex stiffness varying with frequency for different G_p

5 结论

考虑桩周土和桩芯土的粘弹性特性,并借助分数导数 Kelvin 粘弹性模型描述土体的应力-应变关系,研究了分数导数粘弹性土中管桩的扭转振动。得到以下主要结论:

1) 桩周土本构模型参数 α_1 和 T_{b1} 对管桩的振动的影较大,而桩芯土本构模型参数 T_{b2} 和 α_2 对管桩的扭转振动的影响与频率有关,即高频时有影响低频时几乎没有影响。

2) 桩芯土与桩周土剪切模量比 μ 大于 1 和小于 1 时对管桩桩顶扭转复刚度的影响规律不同,当桩芯土剪切模量较小时需要考虑桩周土和桩芯土力学性质的差异的影响。

3) 管桩内外半径比和长径比等几何特性和桩土模量比等力学特性对管桩扭转振动影响较大,需要重点考虑。

参考文献:

[1] NOVAK M, ABOULELLA F. Impedance functions of piles in layered media [J]. Journal of Engineering Mechanical Division, 1978, 104(3): 643-661.
 [2] NOGAMI T, KONAGAI K. Time domain flexural response of dynamically loaded single pile [J]. Journal of Engineering Mechanics, 1988, 114(9): 1512-1525.
 [3] 王国才,王哲,陈龙珠,等. 均匀弹性地基中单桩的扭转振动特性研究[J]. 岩土力学, 2008, 29(11): 3027-3036.
 WANG G C, WANG Z, CHEN L Z, et al. Research on torsional oscillation characteristics of single pile embedded

- in isotropic elastic foundation [J]. *Rock and Soil Mechanics*, 2008, 29(11): 3027-3036. (in Chinese)
- [4] LÜ S H, WANG K H, WU W B. Longitudinal vibration of pile in layered soil based on Rayleigh-Love rod theory and fictitious soil-pile model [J]. *Journal of Central South University*, 2015, 22(5): 1909-1918.
- [5] 刘林超, 闫启方, 王颂, 等. 基于轴对称模型的管桩竖向振动研究[J]. *岩土力学*, 2016, 37(1): 119-125.
LIU L C, YAN Q F, WANG S, et al. Vertical vibration of pipe pile based on axisymmetric model [J]. *Rock and Soil Mechanics*, 2016, 37(1): 119-125. (in Chinese)
- [6] 栾鲁宝, 丁选明, 刘汉龙, 等. 考虑剪切变形的PCC桩水平振动响应解析解[J]. *岩石力学与工程学报*, 2016, 35(11): 2345-2358.
LUAN L B, DING X M, LIU H L, et al. Analytical solutions to lateral dynamic response of PCC piles considering shear deformation [J]. *Chinese Journal of Rock Mechanics and Engineering*, 2016, 35(11): 2345-2358. (in Chinese)
- [7] 吴文兵, 邓国栋, 张家生, 等. 考虑横向惯性效应时桩侧土-管桩-土塞纵向耦合振动特性研究[J]. *岩土力学*, 2017, 38(4): 993-1001.
WU W B, DENG G D, ZHANG J S, et al. Vertical dynamic response of soil surrounding pipe-pile-soil plug by considering lateral inertial effect [J]. *Rock and Soil Mechanics*, 2017, 38(4): 993-1001. (in Chinese)
- [8] NOVAK M. Dynamic stiffness and damping of piles [J]. *Canadian Geotechnical Journal*, 1974, 11(4): 574-598.
- [9] YAO S, NOGAMI T. Lateral cyclic response of a pile in viscoelastic Winkler subgrade [J]. *Journal of Engineering Mechanics*, 1994, 120(4): 758-775.
- [10] 周绪红, 蒋建国, 邹银生. 粘弹性介质中考虑轴力作用时桩的动力分析[J]. *土木工程学报*, 2005, 38(2): 87-91.
ZHOU X H, JIANG G, ZHOU Y S. Dynamic analysis of piles under axial loading and lateral dynamic force in viscoelastic medium [J]. *China Civil Engineering Journal*, 2005, 38(2): 87-91. (in Chinese)
- [11] 杨骁, 刘慧, 蔡雪琼. 端承粘弹性桩纵向振动的轴对称解析解[J]. *固体力学学报*, 2012, 33(4): 423-430.
YANG X, LIU H, CAI X Q. Axisymmetrical analytical solution for vertical vibration of end-bearing viscoelastic pile [J]. *Chinese Journal of Solid Mechanics*, 2012, 33(4): 423-430. (in Chinese)
- [12] 郑长杰, 刘汉龙, 丁选明, 等. 饱和黏性土地基中现浇大直径管桩水平振动响应解析解[J]. *岩土工程学报*, 2014, 36(8): 1447-1454.
ZHENG C J, LIU H L, DING X M, et al. Analytical solution of horizontal vibration of cast-in-place large-diameter pipe piles in saturated soils [J]. *Chinese Journal of Geotechnical Engineering*, 2014, 36(8): 144-1454. (in Chinese)
- [13] 郑长杰, 丁选明, 栾鲁宝. 黏弹性地基中管桩水平动力特性分析[J]. *岩土力学*, 2017, 38(1): 1-8.
ZHANG Z Q, DING X M, LUAN L B. Study on the lateral dynamic response of a pipe pile in viscoelastic soil layer [J]. *Rock and Soil Mechanics*, 2017, 38(1): 1-8. (in Chinese)
- [14] 吴文兵, 蒋国盛, 邓国栋, 等. 黏弹性地基中基于虚土桩模型的桩顶纵向振动阻抗研究[J]. *振动与冲击*, 2015, 34(7): 192-203.
WU W B, JIANG G S, DENG G D, et al. Vertical dynamic impedance of pile embedded in viscoelastic soil based on fictitious soil pile model [J]. *Journal of Vibration and Shock*, 2015, 34(7): 192-203. (in Chinese)
- [15] 刘林超, 张卫. 具有分数 Kelvin 模型的粘弹性岩体中水平圆形洞室的变形特性[J]. *岩土力学*, 2005, 26(2): 287-289.
LIU L C, ZHANG W. The deformation proprieties of horizontal round adits in viscoelastic rocks by fractional Kelvin model [J]. *Rock and Soil Mechanics*, 2005, 26(2): 287-289. (in Chinese)
- [16] 刘林超, 闫启方. 分数导数模型描述的粘弹性土层中桩基水平振动研究[J]. *工程力学*, 2011, 28(12): 139-145.
LIU L C, YAN Q F. Lateral vibration of single pile in viscoelastic soil described by fractional derivative model [J]. *Engineering Mechanics*, 2011, 28(12): 139-145. (in Chinese)
- [17] 刘林超, 杨骁. 分数导数模型描述的饱和土桩纵向振动分析[J]. *岩土力学*, 2011, 32(2): 526-532.
LIU L C, YANG X. Analysis of vertical vibrations of a pile in saturated soil described by fractional derivative model [J]. *Rock and Soil Mechanics*, 2011, 32(2): 526-532. (in Chinese)
- [18] 闻敏杰, 徐金明, 李强. 饱和黏弹性土中端承桩扭转振动的对比分析[J]. *浙江大学学报(工学版)*, 2013, 47(12): 2146-2152.
WEN M J, XU J M, LI Q. Comparative analysis for torsional vibration of an end-bearing pile in saturated viscoelastic soil [J]. *Journal of Zhejiang University*, 2013, 47(12): 2146-2152. (in Chinese)
- [19] TIMOSHENKO S P. *Theory of elasticity* [M]. New York: McGraw-Hill Book, 1934.
- [20] BAGLEY R L, TORVIK P J. A theoretical basis for the application of fractional calculus to viscoelasticity [J]. *Journal of Rheology*, 1983, 27(3): 201-210.
- [21] MILLER K S, ROSS B. *An introduction to the fractional calculus and fractional differential equations* [M]. New York: Wiley, 1993.
- [22] 孙海忠, 张卫. 一种分析软土黏弹性的分数导数开尔文模型[J]. *岩土力学*, 2007, 28(9): 1983-1986.
SUN H Z, ZHANG W. Analysis of soft soil with viscoelastic fractional derivative Kelvin model [J]. *Rock and Soil Mechanics*, 2007, 28(9): 1983-1986. (in Chinese)